

Zones of quiet in a broadband diffuse sound field

Boaz Rafaely

Institute of Sound and Vibration Research

University of Southampton, Southampton, SO17 1BJ, UK

3 April, 2001

Abbreviated title: Broadband zones of quiet

Corresponding author:

Boaz Rafaely

Institute of Sound and Vibration Research

University of Southampton,

Southampton, SO17 1BJ

UK

Email: br@isvr.soton.ac.uk

Tel: +44 (0)23 80593043

Fax: +44 (0)23 80593190

Abstract

The zones of quiet in pure-tone diffuse sound fields have been studied extensively in the past, both theoretically and experimentally, with the well known result of the 10 dB attenuation extending to about a tenth of a wavelength. Recent results on the spatial-temporal correlation of broadband diffuse sound fields are used in this study to develop a theoretical framework for predicting the extension of the zones of quiet in broadband diffuse sound fields. This can be used to study the acoustic limitations imposed on local active sound control systems such as an active headrest when controlling broadband noise. Spatial-temporal correlation is first revised, after which derivations of the diffuse field zones of quiet in the near-field and the far-field of the secondary source are presented. The theoretical analysis is supported by simulation examples comparing the zones of quiet for diffuse fields excited by tonal and broadband signals. It is shown that as a first approximation the zone of quiet of a low-pass filtered noise is comparable to that of a pure-tone with a frequency equal to the center frequency of the broadband noise bandwidth.

PACS numbers: 43.50.Ki, 43.55.Cs

1 Introduction

Active control of sound has been studied intensively in the past two decades, both theoretically and experimentally^{1,2}. Global control of sound in enclosures was shown to be limited to the very low frequencies, where only few acoustic modes dominate the sound field¹, and so in many cases active control is practical only locally, generating limited zones of quiet. A typical application for local active sound control is a noise reducing headrest in a passenger seat, attenuating noise around the passenger's ears^{3,4,5,6,7,8}. Since local control would usually be performed in enclosures, a model which was often used is that of diffuse primary sound field, and a decaying near field to model the secondary pressure from a closely located source. Pure-tone sound fields have been studied extensively for such local control, developing theoretical limits on the spatial extension of the zone of quiet^{9,10}, and verifying the results with experiments⁸. It was shown that the 10 dB zone of quiet is extended to about tenth of a wavelength for pure-tone sound fields¹¹. The analysis of zones of quiet in diffuse fields used the well-known spatial correlation function of pure-tone diffuse fields^{9,10}, derived by Cook *et al.* in the 50's¹².

Although the theoretical and experimental results for pure-tone local control were useful to predict the performance of active headrest attenuating low frequency tonal noise in propeller aircraft, for example, in many cases the nature of the noise is broadband, such as in most jet passenger aircraft, and so pure-tone results will be of limited use in this case. For a broadband local active control system a useful measure of performance would be the spatial extent of the overall sound attenuation, which requires the analysis of broadband sound fields and so cannot make use of the pure-tone results. Previous studies of broadband local control systems were performed experimentally, by including, for example, the effect of the feedback control system, which would usually be used in this case^{4,5}. It was shown that broadband local active control could be useful in practice, although in addition to the limitations imposed

by the acoustics, other limitations are also imposed by the control system, due to, for example, the delay in the response between the loudspeaker and the cancellation point.

The aim of this paper is to develop a theoretical framework for predicting the spatial extent of the zones of quiet in broadband diffuse sound fields. This can then be used to predict performance limitations of broadband active headrest systems as imposed by the acoustics, and can complement previous experimental results. Similar to the pure-tone zones of quiet case, the analysis of broadband zones of quiet presented here employ spatial correlation of diffuse sound fields. However, in this work *broadband* spatial-temporal correlation is used, as developed recently by Rafaely¹⁵.

The paper is organized as follows. First the diffuse sound field and spatial correlation are introduced, after which theoretical results for broadband local control are developed, for near-field control, but also for far-field control, where the secondary source is located away from the cancellation point. Finally simulation results for various broadband sound fields are presented and compared to the pure-tone case. It is shown that as a first approximation, broadband zone of quiet can be predicted from that of tones at the mid-frequency of the broadband noise bandwidth.

2 The Diffuse sound field

The plane wave model of a diffuse sound field assumes an infinite number of plane waves, arriving uniformly from all directions, with random phases^{16,17}. Although a perfect diffuse fields rarely exists, the model is widely used for reverberant sound fields analysis, where the field is assumed to be sufficiently diffuse. A commonly used definition for sufficiently diffuse field is that by Schroeder¹⁸, which defines the field being diffuse above the Schroeder frequency. This corresponds to the frequency above which there exists at least three room modes within the 3 dB bandwidth of any one

mode¹⁶. This complements the wave model of a diffuse field if it is assumed that each mode can be represented by eight plane waves¹⁹, and so a large number of significant modes implies a large number of plane waves, which in the limit approaches the definition of a perfect diffuse field. The pressure in a perfect diffuse field can therefore be written as a function of space and time in spherical coordinates $\mathbf{r} = (r, \theta, \phi)$ as¹⁶:

$$p(\mathbf{r}, t) = \lim_{N \rightarrow \infty} \frac{1}{N} \sum_{n=1}^N p_n(\mathbf{r}, t) \quad (1)$$

where $p(\mathbf{r}, t)$ is the total pressure at position \mathbf{r} and time t , N is the number of plane waves which approaches infinity, and p_n is the n 'th plane wave. The spatial correlation in pure tone diffuse field was studied both theoretically and experimentally by Cook *et al.*¹², who showed that it behaves as a sinc function,

$$\rho(\Delta\mathbf{r}) = \text{sinc}(k\Delta\mathbf{r}) = \frac{\sin(k\Delta\mathbf{r})}{k\Delta\mathbf{r}} \quad (2)$$

where k denotes the wave number, and ρ the correlation coefficient, which can be defined, assuming the sound field is stationary over both space and time¹, as:

$$\rho(\Delta\mathbf{r}, \Delta t) = \frac{E[p(\mathbf{r}_1, t_1)p(\mathbf{r}_0, t_0)]}{E[p^2]} \quad (3)$$

where $\Delta\mathbf{r}$ denotes the distance between the two points, $\Delta\mathbf{r} = |\mathbf{r}_1 - \mathbf{r}_0|$, Δt denotes the time lag given by $\Delta t = t_1 - t_0$, $E[\cdot]$ denotes the expectation operation which is calculated as the average over many samples of diffuse sound fields, and $E[p^2]$ is the variance of the pressure which is not dependent on \mathbf{r} or t due to the stationarity assumption. As discussed above, (2) was widely used in the theoretical analysis of zones of quiet in pure-tone diffuse sound fields. Rafaely¹⁵, recently developed an expression for the correlation which can incorporate both pure-tone and broadband sound fields, and which depends on the power spectral density of the signal exciting the diffuse field,

$$\rho(\Delta\mathbf{r}, \Delta t) = \frac{1}{2\pi E[p^2]} \int_{-\infty}^{\infty} S(\omega) \text{sinc}\left(\frac{\omega\Delta\mathbf{r}}{c}\right) e^{j\omega\Delta t} d\omega \quad (4)$$

where $E[p^2]$ is equal to the integral over $S(\omega)$, i.e. the signal power. Equation (4) enables the extension of the pure-tone local control results to broadband sound fields, as shown in the following sections.

3 Near-field broadband active sound control

Local active sound control in a diffuse sound field can be achieved by introducing a secondary source and cancelling the total pressure in the near-field of the source. A simple model used to theoretically study such an approach is that of a monopole secondary source in a primary diffuse sound field. This arrangement was used by Joseph *et al.*¹⁰ to study zones of quiet in pure-tone diffuse fields, and provided a useful insight into the performance of more practical near-field active sound control systems such as an active headrest system. A derivation of the spatial extension of the zones of quiet in *broadband* diffuse sound field for local active control is presented in this section. This is a novel result which can be used to predict the spatial extent of the overall attenuation of the broadband noise in diffuse sound fields.

Consider a secondary monopole source placed at the origin of a spherical coordinate system, $\mathbf{r} = (r, \theta, \phi)$, with the resulting pressure denoted by $p_s(\mathbf{r}, t)$. The primary sound field is diffuse and is denoted by $p_p(\mathbf{r}, t)$. The total pressure is a superposition of the primary and secondary pressure contributions and is given by

$$p(\mathbf{r}, t) = p_p(\mathbf{r}, t) + p_s(\mathbf{r}, t) \quad (5)$$

The pressure at position $\mathbf{r}_0 = (r_0, \theta_0, \phi_0)$ is cancelled, i.e. \mathbf{r}_0 is assumed to be the cancellation point, such that

$$p_p(\mathbf{r}_0, t) + p_s(\mathbf{r}_0, t) = 0 \quad (6)$$

It is now assumed that position \mathbf{r}_0 is in the near field of the secondary source, such that the indirect secondary sound field resulting from reflections is negligible.

The distance from the source at which the direct field dominates is referred to as the "reverberation distance", which depends on the room volume and reverberation time¹⁸. The spatial extent of the zone of quiet depends on how well the primary pressure is attenuated around the cancellation point. The averaged squared total pressure at position $\mathbf{r}_1 = (r_1, \theta_1, \phi_1)$ near the cancellation point is therefore calculated, where the expectation operation $E[\cdot]$ is used as a statistical average over many samples of diffuse sound fields. The variance of the total pressure at position \mathbf{r}_1 can therefore be written using (5) as

$$E[p^2(\mathbf{r}_1, t)] = E[p_p^2(\mathbf{r}_1, t)^2] + E[p_s^2(\mathbf{r}_1, t)] + 2E[p_p(\mathbf{r}_1, t)p_s(\mathbf{r}_1, t)] \quad (7)$$

Note that the variance of the total pressure at \mathbf{r}_1 depends on the variance of the primary and secondary fields at the same point, but also on the correlation between the primary and secondary fields at \mathbf{r}_1 . Since we assumed in (6) that both fields are equal with opposite phase at the cancellation point \mathbf{r}_0 , this correlation will depend on how both fields change from \mathbf{r}_0 to \mathbf{r}_1 , which will be developed later. We next expand each of the terms in equation (7), and reformulate the equation.

Assuming the diffuse primary sound field is stationary, such that the variance of the pressure is the same for all \mathbf{r} and t , the following equality can be written

$$E[p_p^2(\mathbf{r}_1, t)] = E[p_p^2(\mathbf{r}_0, t)] = E[p_p^2] \quad (8)$$

It is now assumed that the secondary source is generated by a monopole point source. Although the monopole source is not an accurate representation of more practical secondary sources such as loudspeakers, under some assumptions the pressure produced by a monopole behaves in a similar way to that produced by a piston in a baffle, which is often used to model sound radiation from loudspeakers. These assumptions are²⁰: (1) $ka < 0.5$, or $a < \frac{\lambda}{4\pi}$, which means that the source radius a is much smaller than a wavelength, and the source can therefore be considered

omni-directional, and (2) $r > a$, which suggests that only pressure further away than one source radius is considered. For example, these assumption will hold for a 4 inch ($a = 5$ cm) loudspeaker, for frequencies below about 500 Hz, further than 5 cm from loudspeaker. These are reasonable assumptions considering a practical local active control system such as active headrest^{4,5}, and so the monopole model should provide useful insight into the behaviour of more practical systems.

The secondary sound field produced by a monopole point source in the near-field is assumed to generate spherical waves, which propogate away from the source and decay in amplitude^{19,21}:

$$p_s(r, t) = \frac{\rho_0}{4\pi r} \dot{q} \left(t - \frac{r}{c} \right) \quad (9)$$

which is now dependent only on the distance from the source, r , with q denoting the source strength (volume velocity per unit volume) and \dot{q} its derivative with respect to time. The secondary pressure at \mathbf{r}_1 can now be written in terms of the secondary pressure at \mathbf{r}_0 using (9) as:

$$p_s(\mathbf{r}_1, t) = \frac{r_0}{r_1} p_s \left(\mathbf{r}_0, t - \frac{\Delta r}{c} \right) \quad (10)$$

where $\Delta r = r_1 - r_0$, which is the difference in the distances of the two points \mathbf{r}_1 and \mathbf{r}_0 to the source.

The averaged squared secondary pressure at \mathbf{r}_1 can now be written using (10), (6) and (8) as:

$$\begin{aligned} E[p_s^2(\mathbf{r}_1, t)] &= \left(\frac{r_0}{r_1} \right)^2 E \left[p_s^2 \left(\mathbf{r}_0, t - \frac{\Delta r}{c} \right) \right] \\ &= \left(\frac{r_0}{r_1} \right)^2 E \left[p_p^2 \left(\mathbf{r}_0, t - \frac{\Delta r}{c} \right) \right] = \left(\frac{r_0}{r_1} \right)^2 E[p_p^2] \end{aligned} \quad (11)$$

The last term in (7) can also be written using (10), (6) and (3) as:

$$\begin{aligned}
E[p_p(\mathbf{r}_1, t)p_s(\mathbf{r}_1, t)] &= E\left[p_p(\mathbf{r}_1, t)\frac{r_0}{r_1}p_s\left(\mathbf{r}_0, t - \frac{\Delta r}{c}\right)\right] \\
&= -\frac{r_0}{r_1}E\left[p_p(\mathbf{r}_1, t)p_p\left(\mathbf{r}_0, t - \frac{\Delta r}{c}\right)\right] \\
&= -\frac{r_0}{r_1}\rho\left(\Delta\mathbf{r}, \frac{\Delta r}{c}\right)E[p_p^2] \tag{12}
\end{aligned}$$

The variance of the total pressure at position \mathbf{r}_1 in (7) can now be written in terms of the variance of the primary pressure by substituting equations (8), (11) and (12) in equation (7),

$$E[p^2(\mathbf{r}_1, t)] = E[p_p^2] + \left(\frac{r_0}{r_1}\right)^2 E[p_p^2] - 2\frac{r_0}{r_1}\rho\left(\Delta\mathbf{r}, \frac{\Delta r}{c}\right)E[p_p^2] \tag{13}$$

Dividing (13) by the variance of the primary pressure, an expression for the sound attenuation ϵ at \mathbf{r}_1 assuming cancellation at \mathbf{r}_0 , is derived as follows:

$$\epsilon(\mathbf{r}_1, \mathbf{r}_0) = \frac{E[p^2(\mathbf{r}_1, t)]}{E[p_p^2]} = 1 + \left(\frac{r_0}{r_1}\right)^2 - 2\frac{r_0}{r_1}\rho\left(\Delta\mathbf{r}, \frac{\Delta r}{c}\right) \tag{14}$$

where the sound attenuation in dB is given by $10 \log_{10} \epsilon$. It is important to note that in (14) $\Delta\mathbf{r} = |\mathbf{r}_1 - \mathbf{r}_0|$ is the distance from position \mathbf{r}_1 to the cancellation point \mathbf{r}_0 , while $\Delta r = r_1 - r_0$ is the difference between the distances of the two points \mathbf{r}_1 and \mathbf{r}_0 to the secondary source, as illustrated in Fig. 1. In the simplified case of on-axis attenuation, the two distances are equal, i.e. $\Delta\mathbf{r} = \Delta r$. Equation (14) together with the expression for the spatial-temporal correlation function in a diffuse field (equation (4)), can be used to calculate the attenuation of broadband noise in the near-field of a monopole point source, a distance $\Delta\mathbf{r}$ away from the cancellation point. Examples of near-field zones of quiet in a broadband diffuse sound field are presented below.

4 Far-field broadband active sound control

The previous section described active sound control in a diffuse field where the secondary source was placed close to the cancellation point. The latter was therefore in

the near-field of the secondary source, and the derivation that followed employed this assumption. In this section it is assumed that the cancellation point is far from the secondary source, such that the resulting secondary field at the cancellation point is assumed to be diffuse. In practice this means that the cancellation point is further than a "reverberation distance" or "radius of reverberation"¹⁶ away from the secondary source. In this case both the primary and the secondary sound fields are diffuse. Nevertheless, the two diffuse fields are assumed to be uncorrelated, which is achieved in practice if the primary and secondary sources are positioned sufficiently far away from each other (more than a wavelength away for pure-tone fields¹).

Unlike the case of near-field sound control which provides an insight into the performance of practical active sound control systems, such as an active headrest, broadband sound control using a secondary source in the far-field is less practical. This is because a practical feedforward control system will require a good reference of the noise signal in advance, which is rarely available for broadband noise, e.g. jet turbulence noise, while a feedback control system will have poor performance due to the long delay from the secondary source to the cancellation point. It is important to note that such a limitation is not applicable to pure-tone sound fields where system delay does not affect performance. In addition, placing the secondary source far from the cancellation point could result in large increase in the pressure at other locations in the enclosure¹, which is an undesirable side-effect. Although of less practical relevance, the derivation of far-field broadband active sound control is presented here for theoretical completeness.

Joseph¹⁴ derived an equation for the average mean square pressure away from the cancellation point under similar conditions but when a pure-tone sound field was assumed¹,

$$E[p^2(\mathbf{r}_1)] = (E[p_p^2] + E[p_s^2]) (1 - \rho^2(\Delta\mathbf{r})) \quad (15)$$

The sound attenuation can now be derived, by dividing (15) with the variance of the primary pressure

$$\epsilon(\Delta\mathbf{r}) = \frac{E[p^2(\mathbf{r}_1)]}{E[p_p^2]} = \left(1 + \frac{E[p_s^2]}{E[p_p^2]}\right) (1 - \rho^2(\Delta\mathbf{r})) \quad (16)$$

Elliott *et al.*⁹ noted that the value of $E[p_s^2]/E[p_p^2]$ can only be defined in statistical terms, and does not have a finite mean value. In practice, however, the secondary source strength will be limited, and in an example simulation⁹, a value of $E[p_s^2]$ was used which is three time larger than $E[p_p^2]$, and so for this example (16) can be written as:

$$\epsilon(\Delta\mathbf{r}) = 4(1 - \rho^2(\Delta\mathbf{r})) \quad (17)$$

Equation (4) can now be used in (17) to compute the attenuation or the extent of the far-field zones of quiet for a broadband sound field. Examples of such zones of quiet are presented below.

5 Examples of near-field zones of quiet

Examples of near-field zones of quiet calculated using the results derived above are presented in this section. The primary field is assumed to be diffuse while the secondary field is excited by a monopole point source. The cancellation point where both fields are equal but opposite in phase is located in the near field of the monopole source. A pure-tone diffuse sound field, which has been well studied previously, is compared to broadband diffuse sound fields using the results derived in this work. The diffuse sound fields in the examples presented here are excited by the signals as described in Table 1.

Signal	Description
300 Hz Tone	A 300 Hz pure tone
300 Hz LPF	Broadband signal generated by passing white noise through a 32 nd order Butterworth low-pass filter with a cut-off frequency of 300 Hz
600 Hz LPF	Broadband signal generated by passing white noise through a 32 nd order Butterworth low-pass filter with a cut-off frequency of 600 Hz
BPF	Broadband signal generated by passing white noise through an 8 th order Butterworth low-pass filter with a cut-off frequency of 400 Hz, and another 2 nd order Butterworth high-pass filter with a cut-off frequency of 600 Hz, as used by Rafaely <i>et al.</i> ⁴ to analyze the performance of a laboratory active headrest system

Table 1. Description of the signals used in the simulation examples.

Figure 2 shows the power spectral density of the signals used in the simulation examples as described in Table 1. The spatial correlation of the various primary diffuse sound fields are compared next, after which the correlation functions between the primary and secondary sound fields away from the cancellation point are evaluated, which then leads to a comparison of the zones of quiet. The spatial-temporal correlation function for the pressure in a diffuse sound field is calculated in MATLAB using (4) by generating the appropriate signals, sampled at $F_s = 2$ kHz, with discrete power spectral densities calculated using the discrete Fourier transform (DFT) having $M = 4096$ points. The integral in (4) was approximated by a summation over frequency, as follows:

$$\rho(\Delta \mathbf{r}, \Delta t) \approx \frac{1}{\sum_{m=0}^{M-1} S(m)} \sum_{m=0}^{M-1} S(m) \text{sinc} \left(\frac{2\pi m F_s}{M} \frac{\Delta \mathbf{r}}{c} \right) e^{j \frac{2\pi m F_s}{M} \Delta t} \quad (18)$$

Figure 3 shows the spatial correlation of the primary diffuse field $\Delta\mathbf{r}$ away from the cancellation point, evaluated using (18) as $\rho(\Delta\mathbf{r}, 0)$, for the sound fields described in Table 1. The figure shows that the spatial correlation for the 300 Hz pure-tone sound field behaves as a spatial sinc function, as expected¹², with the 600 Hz low-pass filtered noise having similar correlation for small $\Delta\mathbf{r}$. This observation that the spatial correlation for a band of frequencies can be approximated by that of a pure tone at the center frequency has been previously observed^{12,13}. The 300 Hz low-pass filtered noise has higher spatial correlation, as expected, since it is composed of lower frequencies. It is also interesting to note that the sound field composed of the band-pass filtered noise has a similar spatial correlation to the 600 Hz low-pass filtered noise, for small $\Delta\mathbf{r}$, since it has a similar bandwidth.

As shown in (7), the cross-correlation between the primary diffuse field and the secondary near field when evaluated at \mathbf{r}_1 , i.e. $\Delta\mathbf{r}$ away from the cancellation point, is used in the calculation of the total pressure and then the attenuation at \mathbf{r}_1 . This cross-correlation is evaluated here for the sound fields described in Table 1, using (12) and (18), by substituting $\Delta\mathbf{r}$ and $\Delta t = \frac{\Delta r}{c}$ in the spatial-temporal correlation function of the primary diffuse field. Figure 4 shows this cross-correlation for the signals described in Table 1, where it was assumed that the cancellation point is sufficiently far from the secondary source such that $\mathbf{r}_1 \approx \mathbf{r}_0$ in order to present the limit of the correlation values. The figure shows that the correlation values are negative for small $\Delta\mathbf{r}$ since the primary and secondary fields are equal but with opposite phase at \mathbf{r}_0 . Also, comparing the results to Fig. 3, it is clear that the cross-correlation between the primary and the secondary sound fields at $\Delta\mathbf{r}$ away from the cancellation point is smaller than the auto-correlation of the primary diffuse field for a spacing of $\Delta\mathbf{r}$. This can be explained by the fact that when moving from position \mathbf{r}_0 , where both fields are equal with opposite phase, to position \mathbf{r}_1 , the primary field reduces correlation according to (4), while the secondary field also reduces correlation according to the near-field behaviour described in (10). The total equivalent spacing

between the two fields is therefore $2\Delta\mathbf{r}$, compared to only $\Delta\mathbf{r}$ in Fig. 3, resulting in a greater reduction in the cross-correlation compared to diffuse field auto-correlation.

The attenuation $\Delta\mathbf{r}$ away from the cancellation point can be calculated using (14) and (18). Figure 5 shows the calculated attenuation for the sound fields as described in Table 1, as a function of the distance from the cancellation point $\Delta\mathbf{r}$. Again, it was assumed that $\mathbf{r}_1 \approx \mathbf{r}_0$ to present the limits of the attenuation values. The figure shows that the 300 Hz pure-tone has similar zone of quiet to the 600 Hz low-pass filtered noise and the band-pass filtered noise, whereas the 300 Hz low-pass filtered noise shows larger zones of quiet. It is important to note that the size of the zone of quiet for the 300 Hz pure-tone, defined by $2\Delta\mathbf{r}$ for $\epsilon = 0.1$, i.e. 10 dB attenuation, is about 0.088λ , which is slightly smaller than the 0.1λ rule derived by Nelson and Elliott¹. This is explained by the fact that in the derivation presented in Nelson and Elliott¹ the change in the secondary sound field around the cancellation point was approximated by a first-order function, with higher orders neglected, whereas in this work no such approximation was made.

The 10 dB zone of quiet is presented next, which is the attenuation contour with a 10 dB value. Figure 6 shows the calculated 10 dB attenuation contours, or two-dimensional zones of quiet for the sound fields described in Table 1. In this case the monopole secondary source is located at the origin, while the cancellation point \mathbf{r}_0 is positioned at $(0.2, 0)$, i.e. 20 cm away from the source. The attenuation as a function of position was calculated using (14) and (18), with only the 10 dB attenuation contour shown. The result for the 300 Hz tone is comparable with that of Garcia-Bonito and Elliott⁸, while again it is clear that the 300 Hz tone has similar zone of quiet to the 600 Hz low-pass filtered noise and the band-pass filtered noise. These results suggest that the size of the zone of quiet for a broadband noise of a given bandwidth, will be similar to that of a pure tone at the middle frequency range of the broadband noise. Nevertheless, the zone of quiet for a more general spectrum can be calculated

more accurately as described above.

The 10 dB zone of quiet for the band-pass filtered noise is shown to be about 8 cm. This is slightly higher but comparable to the zone of quiet presented by Rafaely and Elliott⁴, for a laboratory active headrest system, which used a more realistic experiment including a loudspeaker as a source, a Manikin as a head, and feedback control to generate the secondary source signal.

6 Examples of far-field zones of quiet

An example of far-field zones of quiet are presented in this section, where it is assumed that the secondary source is placed far from the cancellation point, such that both the primary field and the secondary field are diffuse. Similar signals as for the previous example were used here to excite the sound fields, which are described in Table 1. Equations (17) and (18) with $\Delta t = 0$ were used to calculate the spatial correlation and then the attenuation for the diffuse sound fields in this example.

Figure 7 show the attenuation as a function of distance from the cancellation point for all four diffuse sound fields. Results are very similar to the near-field case, and here, as well, the zone of quiet for the broadband noise can be approximated by that of a tone at the middle frequency.

7 Conclusions

The zones of quiet for broadband diffuse sound fields were derived theoretically and then demonstrated using simulation examples. Both near-fields zones of quiet, where the cancellation point is in the near-field of the secondary source, and far-field zones of quiet, where the cancellation point is in the far-field of the secondary source, were considered. The paper demonstrated how to calculate the zones of quiet for sound

fields excited by broadband signals, and has presented examples with several low-pass and band-pass type random signals, comparing these to the well known results for tonal excitations. It was shown that for simple low-pass filtered noise, the spatial correlation and the zone of quiet are comparable to those of a tone at the middle bandwidth frequency. Simulation results for near-field zones of quiet for a band-pass noise were comparable to a previous experiment⁴ which used experimental study with a laboratory headrest system. The theory and tools developed here could be used to simulate and predict broadband zones of quiet more accurately in more realistic acoustic configurations which include real sources, a head and a control system, for example, but this is suggested for future work.

References

- [1] P. A. Nelson and S. J. Elliott, *Active control of sound* (Academic Press, London, 1992).
- [2] S. J. Elliott, "Down with noise," *IEEE Spectrum Magazine*, June 1999, 51-61 (1999).
- [3] H. F. Olson and E. G. May, "Electronic sound absorber," *J. Acoust. Soc. Am.* **25**, 1130-1136 (1953).
- [4] B. Rafaely, S. J. Elliott and J. Garcia-Bonito "Broadband performance of an active headrest," *J. Acoust. Soc. Am.* **106**(2), 787-793 (1999).
- [5] B. Rafaely and S. J. Elliott " H_2/H_∞ active control of sound in a Headrest: design and implementation," *IEEE Trans. on Cont. Sys. Tech.* **7**(1), 79-84 (1999).
- [6] J.L. Nielsen, A. Sabo, G. Ottesen, T.A. Reinen and S. Sorsdal, "A local active noise control system for locomotive drivers," *Proceedings of Internoise 2000 conference, Nice, August 2000*, 2901-2905.

- [7] C. Carne, D. Derrien, and G. Valentin, "The ANCAS seat: extentions and industrial applications," Proceedings of ACTIVE 97 conference, Budapest, Hungary, August 1997, 381-390.
- [8] J. Garcia-Bonito and S. J. Elliott, "Local active control of diffracted diffuse sound fields," *Acoust. Soc. Am.* **98**(2), 1017-1024 (1995).
- [9] S. J. Elliott, P. Joseph, A. J. Bullmore, and P. A. Nelson, "Active cancellation at a point in a pure tone diffuse sound field," *Journal of Sound and Vibration*, **120**(1), 183-189 (1988).
- [10] P. Joseph, S. J. Elliott and P. A. Nelson, "Near field zones of quiet," *J. Sound Vibr.*, **172**(5), 605-627 (1994).
- [11] P. Joseph, S. J. Elliott and P. A. Nelson, "Statistical aspects of active control in harmonic enclosed sound fields," *J. Sound Vibr.*, **172**(5), 629-655 (1994).
- [12] R. K. Cook, R. V. Waterhouse, R. D. Berendt, E. Seymour and M. C. Thompson, "Measurement of correlation coefficients in reverberant sound fields," *J. Acoust. Soc. Am.* **27**(6), 1072-1077 (1955).
- [13] H. Nelisse and J. Nicolas, "Characterization of a diffuse field in a reverberant room," *J. Acoust. Soc. Am.* **101**(6), 3517-3524 (1997).
- [14] P. Joseph, "Active control of high frequency enclosed sound fields," PhD Thesis, University of Southampton, England.
- [15] B. Rafaely, "Spatial-temporal correlation of a diffuse sound field," *J. Acoust. Soc. Am.* **107**(6), 3254-3258 (2000).
- [16] A. D. Pierce, *Acoustics - An introduction to its physical principles and application* (McGraw-Hill, New-York, 1981).
- [17] F. Jacobsen, "The diffuse sound field," Report No. 27, The Acoustic Laboratory, Technical University of Denmark (1979).
- [18] M. R. Schroeder "The "Schroeder frequency" revised," *Acoust. Soc. Am.* **99**(5), 3240-3241 (1996).

- [19] L. E. Kinsler, A. R. Frey, A. B. Coppes and J. V. Sanders, *Fundamentals of Acoustics* Third edition, (John Wiley & Sons, New-York, 1982).
- [20] L. L. Beranek, *Acoustics*. American Institute of Physics, NY, (1986).
- [21] P. A. Nelson, J. K. Hammond, P. Joseph and S. J. Elliott "Active control of stationary random sound fields," *J. Acoust. Soc. Am.* **87**(3), 963-975 (1990).

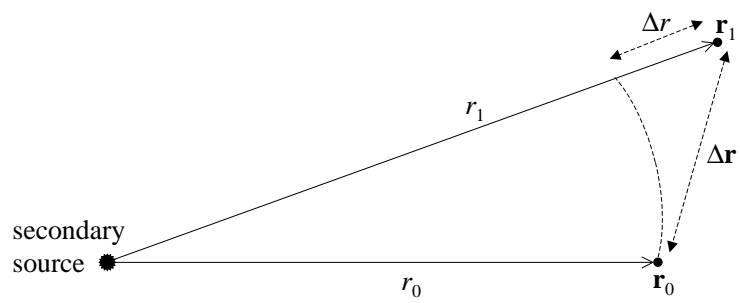


Figure 1: Graphical representation of the cancellation point, \mathbf{r}_0 , and a position near the cancellation point, \mathbf{r}_1 , relative to the secondary source. The distances $\Delta \mathbf{r}$ and Δr are also illustrated in the figure.

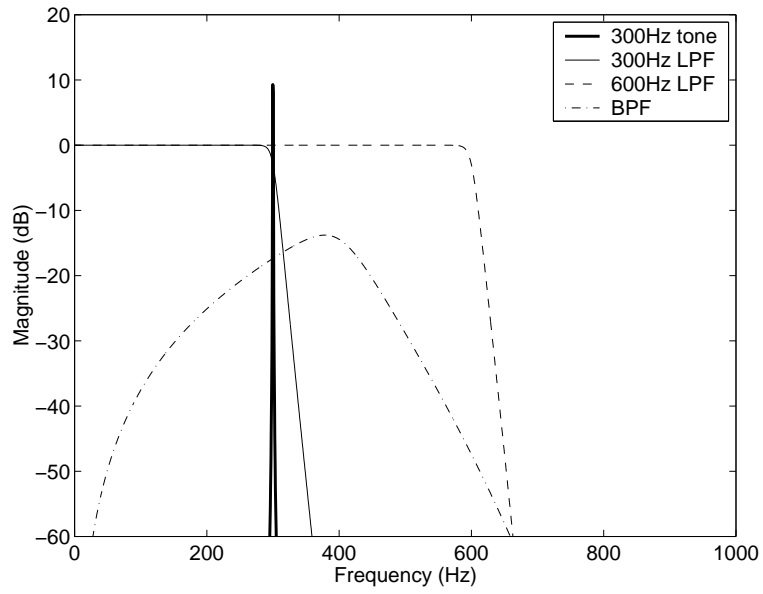


Figure 2: Power spectral density of the signals used in the simulations as described in Table 1.

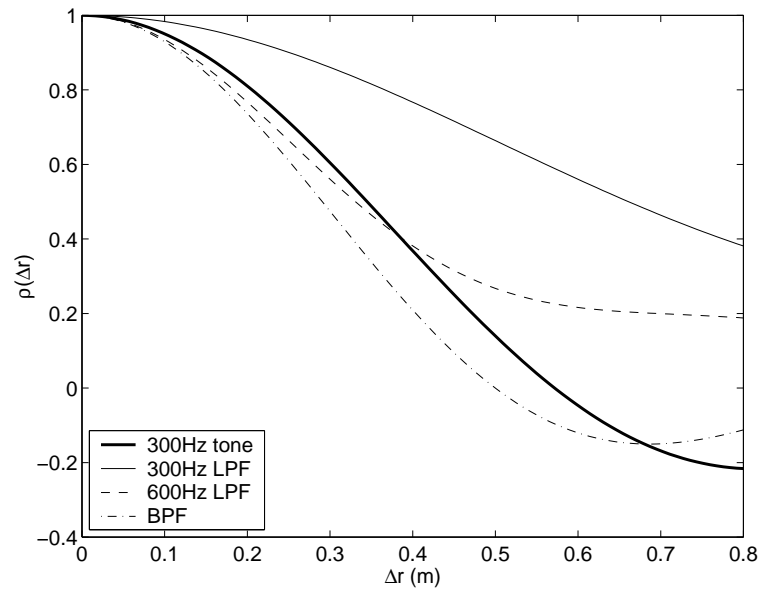


Figure 3: The spatial correlation of the primary pressure in a diffuse sound field, for the excitation signals described in Table 1.

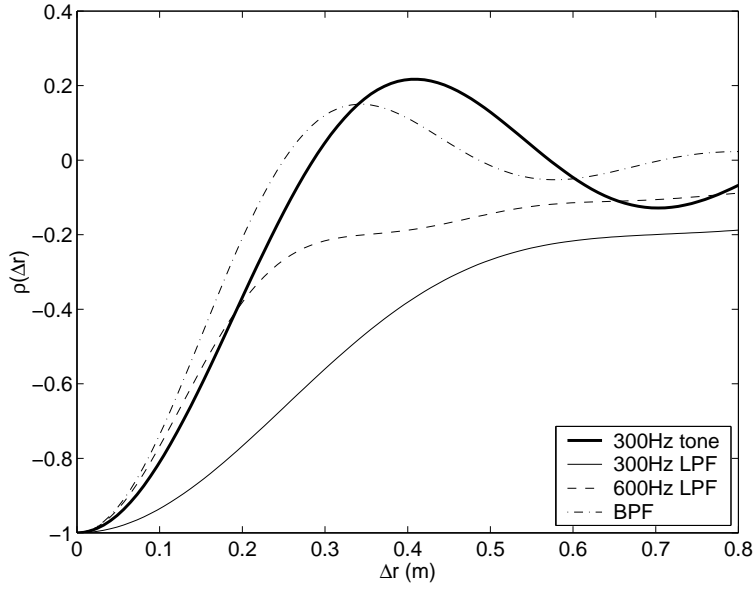


Figure 4: The spatial cross-correlation function between the primary and the secondary pressures $\Delta \mathbf{r}$ away from the cancellation point, $-\frac{r_0}{r_1}\rho(\Delta \mathbf{r}, \frac{\Delta r}{c})$, assuming $\frac{r_0}{r_1} \approx 1$ for the excitation signals described in Table 1.

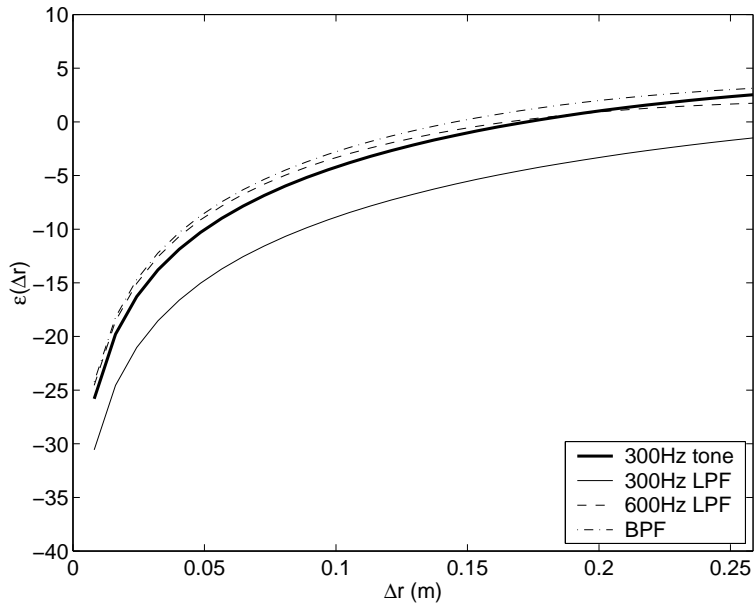


Figure 5: Attenuation as a function of the distance from the cancellation point $\Delta \mathbf{r}$ for the signals described in Table 1.

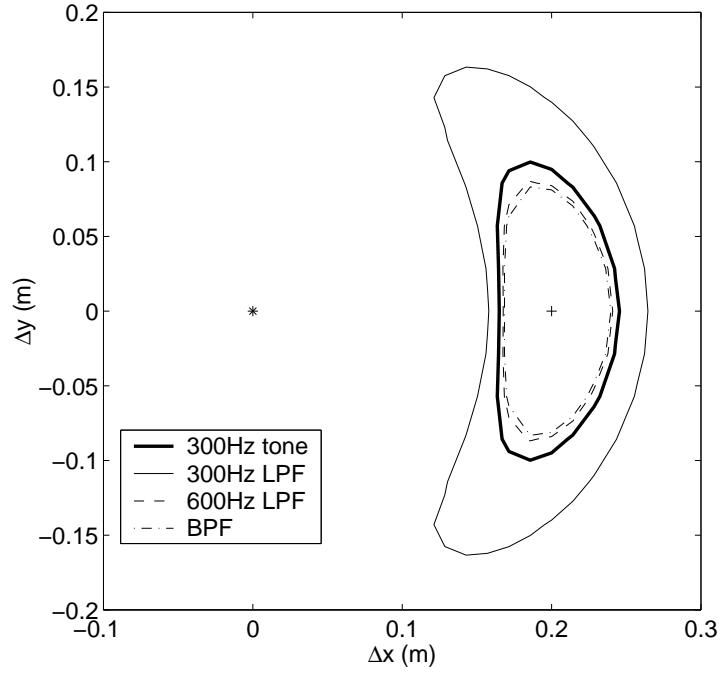


Figure 6: The 10 dB attenuation contours as a function of Δx and Δy , for the signals described in Table 1, with the secondary source denoted by '*' and the cancellation point denoted by '+' located at (0.2, 0).

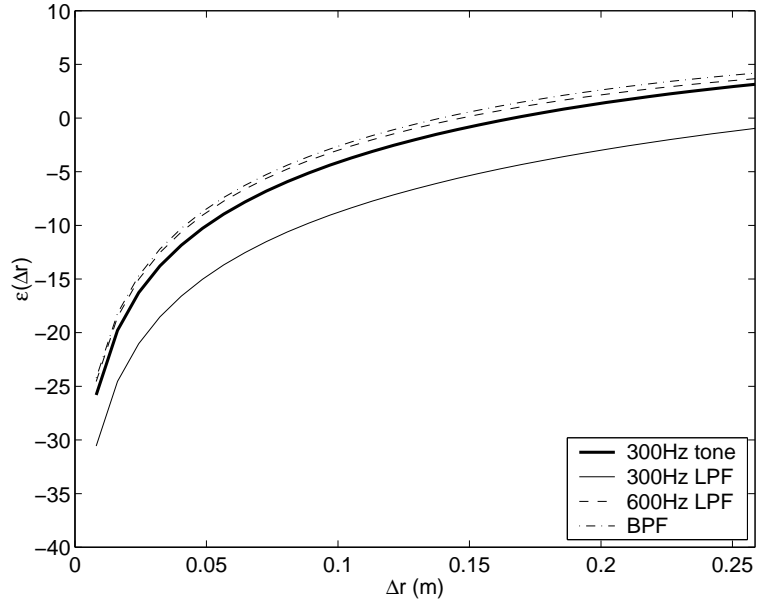


Figure 7: Far-field attenuation as a function of $\Delta \mathbf{r}$, for the signals described in Table 1.